Production cross sections of ^{45}Ti in the deuteron-induced reaction on ^{45}Sc up to 24 MeV

Zolbadral Tsoodol[a,b,*], Masayuki Aikawa[a,c], Dagvadorj Ichinkhorloo[b,c], Tegshjargal Khishigjargal[d], Erdene Norov[d], Yukiko Komori[e], Hiromitsu Haba[e], Sándor Takács[f], Ferenc Ditrói[f], Zoltán Szűcs[f]

[a] *Graduate School of Biomedical Science and Engineering, Hokkaido University, Sapporo 060-8638, Japan*

[b] *Nuclear Research Center, National University of Mongolia, Ulaanbaatar 13330, Mongolia*

[c] *Faculty of Science, Hokkaido University, Sapporo 060-0810, Japan*

[d] *School of Engineering and Applied Sciences, National University of Mongolia, Ulaanbaatar 14201, Mongolia*

[e] *Nishina Center for Accelerator-Based Science, RIKEN, Wako 351-0198, Japan*

[f] *Institute for Nuclear Research (ATOMKI), 4026 Debrecen, Hungary*

Abstract

Activation cross sections of the medically interesting radionuclide ^{45}Ti were investigated in the deuteron-induced reaction on ^{45}Sc. ^{45}Ti can be produced in a radioactive-contamination-free form in the ^{45}Sc(d,2n)^{45}Ti reaction below 15 MeV deuteron energy. The stacked foil activation technique and γ-ray spectrometry were used to determine the cross sections. The physical yield of ^{45}Ti was deduced from the measured cross sections.

Keywords

Titanium-45; Deuteron irradiation; Scandium-45; Excitation function; Cross section; Physical yield

1. Introduction

The radionuclide ^{45}Ti has a half-life of 3.08 h and is a positron emitter ($E_{\beta+}^{max}$ = 1040 keV, $E_{\beta+}^{ave}$ = 439 keV, $I_{\beta+}$ = 84.8%)(National Nuclear Data Center, 2019). The maximum and average energies of emitted positrons are comparable to those from ^{11}C and smaller than those of ^{15}O and appropriate for the small animal PET (Vavere et al., 2005). This PET isotope can be used for investigation of titanium leaking of medical implants (Kim et al., 2019) as well as for the study of the neurotoxicity of titanium dioxide nanoparticles (Song et al., 2015) and in other applications. The deuteron-induced reaction on a monoisotopic ^{45}Sc target is a possible route to produce this radionuclide at low energy cyclotrons. However, only one experimental study (Hermanne et al., 2012) on the cross sections of the ^{45}Sc(d,2n)^{45}Ti reaction was found in our literature survey and their experimental data are scattered. Hence, the main purpose of the present study was to remeasure the cross sections of this reaction with higher confidence. We also measured the cross sections of radioactive by-products, ^{44}Ti and ^{44g,44m,46}Sc. The physical yields for the ^{45}Ti production were also deduced from the measured cross sections.

2. Experimental methods

The experiment was performed at the AVF cyclotron of RIKEN RI Beam Factory. Stacked-foil activation technique and γ-ray spectrometry were used to measure the cross sections.

* Corresponding author at Graduate School of Biomedical Science and Engineering, Hokkaido University, Sapporo 060-8638, Japan.

E-mail address: zolbadral@nds.sci.hokudai.ac.jp (Z.Tsoodol).

The stacked target consisted of metallic foils of ^{45}Sc (25-μm thick, 99.0% purity, Nilaco Corp., Japan and 250-μm thick, 99.9% purity, Johnson Matthey Alfa Products company, USA), ^{27}Al (18-μm thick, 99.6% purity, Nilaco Corp., Japan) and ^{nat}Ti (20-μm thick, 99.6% purity, Nilaco Corp., Japan). The Ti foils served for monitoring the beam parameters via the ^{nat}Ti(d,x)^{48}V reaction. The Al foils were inserted to sandwich the Sc foils and to separate the recoiled reaction products from each Sc and Ti foils. The average thicknesses of the foils were derived by measuring the weights and sizes of larger area foils from the suppliers before cutting them up. The derived thicknesses were 25.8 and 250 μm for ^{45}Sc, 18.5 μm and 20.2 μm for ^{27}Al and ^{nat}Ti, respectively. The foils were cut into the size of 8×8 mm to fit into the target holder, which served as a Faraday cup. The two thicker Sc foils were placed at the top of the stack for cross section measurements of the long-lived ^{44}Ti ($T_{1/2}$ = 59.1 y).

The stacked target was irradiated for 30 min with a deuteron beam of 24.3 ± 0.1 MeV energy, determined by the time-of-flight method (Watanabe et al., 2014). The average intensity of the deuteron beam determined by the collected charge measurement with the Faraday cup-like target holder was 180 nA. The energy degradation in the stacked target was calculated using the SRIM code (Ziegler et al., 2010).

The γ-ray spectra of each irradiated foil were measured by a high-resolution HPGe detector (ORTEC GEM30P4-70) without chemical separation. The detector was calibrated by a mixed γ-ray point source containing ^{57,60}Co, ^{88}Y, ^{109}Cd, ^{113}Sn, ^{137}Cs, ^{139}Ce, and ^{241}Am. Several series of γ-ray measurements were performed to follow the decay of the produced isotopes. The first series of the measurements for short-lived isotopes started after a cooling time of about 1 hour. Each foil was measured more than three times in 5 months. The distance between the detector and the foils was arranged to keep the dead time less than 7%, but each series was always measured with the same detector-sample distance.

The measured γ-ray spectra were analyzed by the Gamma Studio software (SEIKO EG&G). The nuclear reaction and decay data for the γ-ray spectrometry were taken from NuDat 2.8 (National Nuclear Data Center, 2019), LiveChart (International Atomic Energy Agency, 2009; Verpelli and Abriola, 2011) and QCalc (Pritychenko and Sonzongni, 2003), and are listed in Table 1 for all possible contributing reactions for the formation of radionuclides of interest.

The cross sections of the ^{nat}Ti(d,x)^{48}V monitor reaction were used to check the primary beam parameters and target thicknesses. The measurements of the 1312.11 keV γ-rays (I_γ = 98.20%) emitted by the decaying ^{48}V ($T_{1/2}$ = 15.97 d) were performed after a cooling time of 1 month in order to avoid the possible interference from decay of ^{48}Sc ($T_{1/2}$ = 43.67 h). The cross sections derived from the measurements for the ^{nat}Ti(d,x)^{48}V reaction were compared with the IAEA recommended values (Hermanne et al., 2018; Takács et al., 2007) in Fig. 1. The beam intensity determined by the Faraday cup measurement was decreased by 2.0% to have the best agreement between our result and the recommended curve of 2007. The corrected beam intensity (177 nA) was adopted in the data assessment for the cross sections. As the shape of the measured excitation function of the monitor reaction coincided with the shape of the 2007 recommended values, the recent recommended values for the monitor reaction published in 2017 were not used. The measured thicknesses and incident beam energy were used to derive production cross sections.

The initial uncertainty on the incident projectile energy of ± 0.1 MeV is propagated to ± 0.6 MeV in the last foil of the stack, which was estimated from uncertainties of the incident energy and target thicknesses (<2%). The energy degradation of 2.0-2.2 and 0.2-0.6 MeV in thick and thin foils were obtained using the SRIM code. The midpoint projectile energy, energy thickness of each foil and the uncertainties were listed in Table 2. The total uncertainty of the cross sections was 8.1-28.7%. It was estimated as the square root of the quadratic summation of the components; beam

intensity (5%), target thickness, target purity (1%), detector efficiency (6%), γ-intensity (<8%), and γ-ray counting (0.4-26.4%). The statistical uncertainty was high for the very low-intensity γ line of ^{45}Ti (719.6 keV, 0.154%) due to the small peak relative to the background of the gamma-spectra.

3. Results

The activation cross sections of ^{44,45}Ti and ^{44g,44m,46}Sc were determined for the deuteron-induced reactions on ^{45}Sc. The results are summarized in Table 2 and graphically shown in Figs. 2-6, in comparison with the previous experimental data (Hermanne et al., 2012; Skobelev et al., 2011) and the theoretical estimation of TENDL-2019 (Koning et al., 2019). Our results in the figures show the total uncertainties of the projectile energy without the energy thickness and those of the cross sections. Physical yield for the radionuclide ^{45}Ti was derived from the measured cross sections and is shown in Fig.7.

3.1 Formation of ^{45}Ti

As scandium is a monoisotopic element, ^{45}Ti ($T_{1/2}$ = 3.08 h) can be produced in the (d,2n) reaction on ^{45}Sc. The cross sections of the reaction were derived in the measurements after a cooling time of about 1 hour from the low intensity 719.6 keV (I_γ = 0.154%) γ-rays emitted in the decay of ^{45}Ti. The excitation function is shown in Fig. 2 in comparison with the previous data (Hermanne et al., 2012) and the theoretical estimation of TENDL-2019 (Koning et al., 2019). The present cross section data are consistent with the data reported by Hermanne et al. (2012) and are less scattered. The peak position of the TENDL-2019 data is slightly shifted to the lower energy against the two experimental datasets.

3.2 Formation of ^{44}Ti

The long-lived radioisotope ^{44}Ti ($T_{1/2}$ = 59.1 y) can be formed by only the (d,3n) reaction on ^{45}Sc. It decays by EC process (100%) into ^{44g}Sc. After a long cooling time of about 5 months, the γ-ray measurements were performed for more than 6 hours for the first two thicker Sc foils (250 μm thickness). The 78.32-keV γ-rays (I_γ= 96.4%) emitted in the decay of ^{44}Ti were used to derive the cross sections of the ^{45}Sc(d,3n)^{44}Ti reaction. For this low energy γ-rays, the self-absorption correction (Alfassi et al., 2009) was considered using the mass attenuation coefficient of 0.40 cm^2/g for the γ-line at 78.32 keV (Hubbel and Seltzer, 2004). The self-absorption was estimated to be 1.5%. The internal consistency was checked with the 67.87 keV γ-line (I_γ= 93%). The derived cross sections are compared with the previous experimental data (Hermanne et al., 2012) and the theoretical estimation of TENDL-2019 (Koning et al., 2019) in Fig. 3. The energy uncertainty of the two data points of Hermanne et al., 2012 is large because these two points correspond to the last two foils of a long stack irradiated at 50 MeV deuteron energy. Our data agree with the data reported by Hermanne et al. (2012) within the uncertainty. The TENDL-2019 data largely overestimate the two experimental datasets.

3.3 Formation of ^{46}Sc

The short-lived meta-stable state ($T_{1/2}$ = 18.75 s) and the long-lived ground state ($T_{1/2}$ = 83.79 d) of ^{46}Sc can be simultaneously formed by the (d,p) reaction on ^{45}Sc. The meta-stable state decayed by the internal transition (IT) (100%) into the ground state during a cooling time of about 1 week. The cumulative cross sections of the ^{45}Sc(d,p)^{46}Sc reaction were derived from the measurement of the 1120.545-keV γ-line (I_γ = 99.987%) from the decay of the ground state. The excitation function for the ^{46}Sc production is shown in Fig. 4 in comparison with the previous experimental data

(Hermanne et al., 2012; Skobelev et al., 2011), and the TENDL-2019 data (Koning et al., 2019). The present data are consistent with both the experimental data sets. The predictions by TENDL-2019 are lower than those of the experimental data.

3.4 Formation of ^{44m}Sc

The (d,t), (d,dn) and (d,p2n) reactions on ^{45}Sc contribute to the formation of the long-lived meta-stable state of ^{44}Sc ($T_{1/2}$ = 58.61 h). The meta-stable state, ^{44m}Sc decays by the IT process (98.8%) into the ground state ^{44g}Sc and by the EC process (1.2%) into ^{44}Ca. The cross sections of the ^{45}Sc(d,x)^{44m}Sc reaction were derived from the measurements of the intense γ-rays at 271.24 keV (I_γ = 86.7%) emitted from the decay of ^{44m}Sc. The γ-ray spectrometry measurement was performed after an average cooling time of about 28 hours. The excitation function for the ^{45}Sc(d,x)^{44m}Sc reaction is shown in Fig. 5 in comparison with the previous experimental data (Hermanne et al., 2012) and the TENDL-2019 data (Koning et al., 2019). The present dataset is consistent with the data reported by Hermanne et al. (2012). The TENDL-2019 data overestimate the experimental cross sections above 15 MeV.

3.5 Formation of ^{44g}Sc

The ground state of ^{44}Sc ($T_{1/2}$ = 3.97 h) can be formed directly in the ^{45}Sc(d,x)^{44g}Sc process and indirectly by decay of its co-produced meta-stable state ^{44m}Sc. The contribution of the parent nucleus ^{44}Ti is very small and neglected due to its long half-life and small production cross sections, which were derived in section 3.2. The ground state decays by β^+ and EC processes into ^{44}Ca. The intense γ-rays at 1157.02 keV (I_γ = 99.9%) were used in the data assessment. The contributions to the collected counts from both decay processes of ^{44m}Sc to ^{44g}Sc (IT: 98.8%) and ^{44}Ca (EC: 1.2%) were subtracted using the cross sections presented in section 3.4. The estimated contributions of the IT and EC processes of ^{44m}Sc were less than 35% and 0.5%, respectively. Both contributions were subtracted from the measured counts of the 1157.02-keV photo-peak. The corrected net areas were then used to derive the independent cross sections for the ^{45}Sc(d,x)^{44g}Sc reaction. The derived excitation function is shown in Fig. 6 in comparison with the previous experimental data (Hermanne et al., 2012; Skobelev et al., 2011) and the TENDL-2019 prediction (Koning et al., 2019). Our data are between the experimental data reported by Hermanne et al. (2012) and Skobelev et al. (2011). The TENDL-2019 data present a partial agreement with our data.

3.6 Integral Yield

The physical yield of ^{45}Ti was deduced from the spline fitted curve of the measured excitation function presented in section 3.1 according to the yield definition (Otuka and Takács, 2015) and the stopping powers calculated using the SRIM code (Ziegler et al., 2010). The result is shown in Fig. 7 with the single experimental data point at 22 MeV (Dmitriev et al., 1983). Our result is slightly larger than the experimental data.

In the irradiation of ^{45}Sc with a deuteron beam, no other radioactive Ti impurities are produced below the threshold energy of the ^{45}Sc(d,3n)^{44}Ti reaction. Therefore, production of ^{45}Ti without radio-contamination is possible in the ^{45}Sc(d,2n)^{45}Ti reaction in the deuteron energy range up to 15 MeV.

The stable isotope ^{46}Ti can also be formed directly and indirectly through the decay of ^{46}Sc in the corresponding nuclear reactions and affect the specific activity and labeling yield of ^{45}Ti. The ratio of produced numbers of ^{45}Ti to all considered titanium (^{45}Ti+^{46}Ti+^{47}Ti) was estimated using our cross section data for ^{45}Ti and ^{46}Sc and the TENDL-2019 data for ^{46}Ti

and ^{47}Ti. This ratio has a maximum in the energy window from 15 to 8 MeV and is about 0.74 at the end-of-bombardment for a 1h irradiation. The EOB activity reaches 680 MBq for 1h and 1μA irradiation. The minimum energy of the applied energy window was optimized for the higher ratio or activity.

4 Conclusion

The excitation function of the ^{45}Sc(d,2n)^{45}Ti reaction was measured up to 24 MeV. The stacked-foil activation technique and the high-resolution γ-ray spectrometry were used for the cross section measurements. The obtained data were compared with the previous experimental data and the TENDL-2019 prediction. The derived excitation function of the ^{45}Sc(d,2n)^{45}Ti reaction is consistent with the earlier published data of Hermanne et al. (2012). The physical yield deduced from the measured cross sections is slightly larger than the experimental data of Dmitriev et al. (1983). The radioactive-contamination-free ^{45}Ti can be obtained via the ^{45}Sc(d,2n)^{45}Ti reaction in the energy region of 15 - 8 MeV applying chemical separation.

Acknowledgements

The experiment was carried out at RI Beam Factory operated by RIKEN Nishina Center and CNS, University of Tokyo, Japan. This work was supported by "Optimization of accelerator production routes of the new theranostic radioisotopes Sc-47 and Cu-67" under the Japan - Hungary Research Cooperative Program between JSPS and HAS. This work is also supported by JSPS KAKENHI Grant Number 17K07004. Z.Ts. was granted a scholarship by the M-JEED project (Mongolian-Japan Engineering Education Development Program, J11B16). Z.Ts. express the gratitude to Dr. Skobelev for his kind response to the inquiry on his study.

Declarations of interest

None.

References

Alfassi, Z.B., Persico, E., Groppi, F., Bonardi, M.L., 2009. On the photon self-absorption correction for thin-target-yields vs. thick-target-yields in radionuclide production. Appl. Radiat. Isot. 67, 240–242. https://doi.org/10.1016/j.apradiso.2008.10.004

Dmitriev, P.P., Krasnov, N.N., Molin, G.A., 1983. Yields of radioactive nuclides formed by bombardment of a thick target with 22-MeV deuterons. (INDC(CCP)-210/L), International Atomic Energy Agency (IAEA).

Hermanne, A., Adam Rebeles, R., Tarkanyi, F., Takacs, S., Takacs, M.P., Csikai, J., Ignatyuk, A., 2012. Cross sections of deuteron induced reactions on ^{45}Sc up to 50 MeV: Experiments and comparison with theoretical codes. Nucl. Instruments Methods Phys. Res. Sect. B Beam Interact. with Mater. Atoms 270, 106–115. https://doi.org/10.1016/j.nimb.2011.09.002

Hermanne, A., Ignatyuk, A. V., Capote, R., Carlson, B. V., Engle, J.W., Kellett, M.A., Kibédi, T., Kim, G., Kondev, F.G., Hussain, M., Lebeda, O., Luca, A., Nagai, Y., Naik, H., Nichols, A.L., Nortier, F.M., Suryanarayana, S. V., Takács, S., Tárkányi, F.T., Verpelli, M., 2018. Reference Cross Sections for Charged-particle Monitor Reactions. Nucl. Data Sheets 148, 338–382. https://doi.org/10.1016/j.nds.2018.02.009

Hubbel, J.H., Seltzer, S.M., 2004. X-Ray Mass Attenuation Coefficients: NIST Standard Reference Database 126 [WWW

Document]. https://doi.org/10.18434/T4D01F

International Atomic Energy Agency, 2009. LiveChart of Nuclides. [WWW Document]. https://www-nds.iaea.org/livechart/.

Kim, K.T., Eo, M.Y., Nguyen, T.T.H., Kim, S.M., 2019. General review of titanium toxicity. Int. J. Implant Dent. 5, 10. https://doi.org/10.1186/s40729-019-0162-x

Koning, A.J., Rochman, D., Sublet, J.C., Dzysiuk, N., Fleming, M., van der Marck, S., 2019. TENDL: Complete Nuclear Data Library for Innovative Nuclear Science and Technology. Nucl. Data Sheets 155, 1–55. https://doi.org/10.1016/j.nds.2019.01.002

National Nuclear Data Center, 2019. Nuclear structure and decay data on-line library, Nudat 2.8 [WWW Document]. http://www.nndc.bnl.gov/nudat2/

Otuka, N., Takács, S., 2015. Definitions of radioisotope thick target yields. Radiochim. Acta 103, 1–6. https://doi.org/10.1515/ract-2013-2234

Pritychenko, B., Sonzongni, A., 2003. Q-value Calculator (QCalc). [WWW Document]. https://www.nndc.bnl.gov/qcalc/

Skobelev, N.K., Kulko, A.A., Kroha, V., Burjan, V., Hons, Z., Daniel, A. V., Demekhina, N.A., Kalpakchieva, R., Kugler, A., Mrázek, J., Penionzhkevich, Y.E., Piskoř, Š., Šimečková, E., Voskoboynik, E.I., 2011. Excitation functions for the radionuclide 46Sc produced in the irradiation of 45Sc with deuterons and 6He. J. Phys. G Nucl. Part. Phys. 38, 35106. https://doi.org/10.1088/0954-3899/38/3/035106

Song, B., Liu, J., Feng, X., Wei, L., Shao, L., 2015. A review on potential neurotoxicity of titanium dioxide nanoparticles. Nanoscale Res. Lett. 10, 342. https://doi.org/10.1186/s11671-015-1042-9

Takács, S., Király, B., Tárkányi, F., Hermanne, A., 2007. Evaluated activation cross sections of longer-lived radionuclides produced by deuteron induced reactions on natural titanium. Nucl. Instruments Methods Phys. Res. Sect. B Beam Interact. with Mater. Atoms 262, 7–12. https://doi.org/10.1016/j.nimb.2007.05.011

Vavere, A.L., Laforest, R., Welch, M.J., 2005. Production, processing and small animal PET imaging of titanium-45. Nucl. Med. Biol. 32, 117–122. https://doi.org/10.1016/j.nucmedbio.2004.10.003

Verpelli, M., Abriola, D., 2011. Information management tools for evaluated nuclear structure data file (ENSDF) interrogation and dissemination. J. Korean Phys. Soc. 59, 1322–1324. https://doi.org/10.3938/jkps.59.1322

Watanabe, T., Fujimaki, M., Fukunishi, N., Imao, H., Kamigaito, O., Kase, M., Komiyama, M., Sakamoto, N., Suda, K., Wakasugi, M., Yamada, K., 2014. Beam energy and longitudinal beam profile measurement system at the RIBF, in: Proceedings of the 5th International Particle Accelerator Conference (IPAC 2014). pp. 3566–3568.

Ziegler, J.F., Ziegler, M.D., Biersack, J.P., 2010. SRIM - The stopping and range of ions in matter (2010). Nucl. Instruments Methods Phys. Res. Sect. B Beam Interact. with Mater. Atoms 268, 1818–1823. https://doi.org/10.1016/j.nimb.2010.02.091

Figure captions

Fig. 1. The excitation function of the $^{nat}Ti(d,x)^{48}V$ monitor reaction compared with the recommended values (Hermanne et al., 2018; Takács et al., 2007).

Fig. 2. The excitation function of the $^{45}Sc(d,2n)^{45}Ti$ reaction.

Fig. 3. The excitation function of the $^{45}Sc(d,3n)^{44}Ti$ reaction.

Fig. 4. The excitation function of the $^{45}Sc(d,p)^{46}Sc$ reaction.

Fig. 5. The excitation function of the $^{45}Sc(d,x)^{44m}Sc$ reaction.

Fig. 6. The excitation function of the $^{45}Sc(d,x)^{44g}Sc$ reaction.

Fig. 7. The physical yield of ^{45}Ti via the deuteron-induced reaction on ^{45}Sc.

Tables

Table 1

Reactions and decay data for the investigated reaction products (International Atomic Energy Agency, 2009; National Nuclear Data Center, 2019; Pritychenko and Sonzongni, 2003). γ-lines in bold were used in our data evaluation.

Nuclide	Half-life	Decay mode [%]	E_γ [keV]	I_γ [%]	Contributing reaction	Q-value [MeV]	Reference
^{45}Ti	3.08 h	ε+β^+ (100)	**719.6**	**0.154(12)**	^{45}Sc(d,2n)	-5.07	Burrows, 2008
^{44}Ti	59.1 y	ε (100)	67.8679 **78.3234**	93.0(2) **96.4(17)**	^{45}Sc(d,3n)	-14.6	Chen et al., 2011
^{46}Sc	83.79 d	β^- (100)	889.277 **1120.545**	99.984(1) **99.987(1)**	^{45}Sc(d,p)	6.5	Wu, 2000
^{44m}Sc	58.61 h	ε (1.2) IT (98.8)	**271.241** 1157.002	**86.7(3)** 1.20(7)	^{45}Sc(d,t) ^{45}Sc(d,dn) ^{45}Sc(d,p2n) ^{44}Ti decay	-5.07 -11.38 -13.55	Chen et al., 2011
^{44g}Sc	3.97 h	ε+β^+ (100)	**1157.02**	**99.9(4)**	^{45}Sc(d,t) ^{45}Sc(d,dn) ^{45}Sc(d,p2n) ^{44m}Sc decay	-5.07 -11.38 -13.55	Chen et al., 2011
^{48}V	15.97 d	ε+β^+ (100)	944.13 983.52 **1312.11**	7.870(7) 99.98(4) **98.20(3)**	^{46}Ti(d,γ) ^{47}Ti(d,n) ^{48}Ti(d,2n) ^{49}Ti(d,3n)	13.5 4.6 -7.0 -15.2	Burrows, 2006

Table 2

Cross sections of ^{44,45}Ti and ^{44m,44g,46}Sc measured in the deuteron bombardment on ^{45}Sc. The midpoint projectile energy, energy thickness of each foil and the uncertainties propagated from those of the incident energy and target thicknesses are shown in the first column.

Energy (MeV)	Cross sections (mb)				
	^{45}Sc(d,2n)^{45}Ti	^{45}Sc(d,3n)^{44}Ti	^{45}Sc(d,p)^{46}Sc	^{45}Sc(d,x)^{44m}Sc	^{45}Sc(d,x)^{44g}Sc
23.3 ±1.0 ± 0.1	237 ± 64	7.44 ±0.71	81.6 ± 6.9	107 ± 9	113 ± 13
20.6 ±1.1 ± 0.1	251 ± 46	3.36 ±0.35	104 ± 9	40.7 ± 3.3	49.7 ± 5.7
18.7 ±0.1 ± 0.2	272 ± 40		102 ± 8	12.3 ± 0.9	17.6 ± 2.1
17.5 ±0.1 ± 0.2	279 ± 43		109 ± 9	5.55 ± 0.46	9.74 ± 1.2
16.3 ±0.1 ± 0.2	297 ± 41		127 ± 10	3.16 ± 0.26	6.57 ± 1.03
14.9 ±0.1 ± 0.2	296 ± 38		143 ± 12	2.11 ± 0.17	4.44 ± 0.85
13.5 ±0.2 ± 0.3	291 ± 36		163 ± 13	1.68 ± 0.14	3.14 ± 0.66
11.9 ±0.2 ± 0.3	261 ± 32		199 ± 16	1.20 ± 0.10	1.96 ± 0.16
10.2 ±0.2 ± 0.3	201 ± 24		253 ± 21	0.539 ± 0.045	0.892 ± 0.075
8.2 ±0.2 ± 0.4	96.5 ± 12.1		316 ± 26	0.104 ± 0.012	0.194 ± 0.018
5.8 ±0.3 ± 0.6	3.14 ± 0.54		311 ± 25	0.074 ± 0.009	0.130 ± 0.011

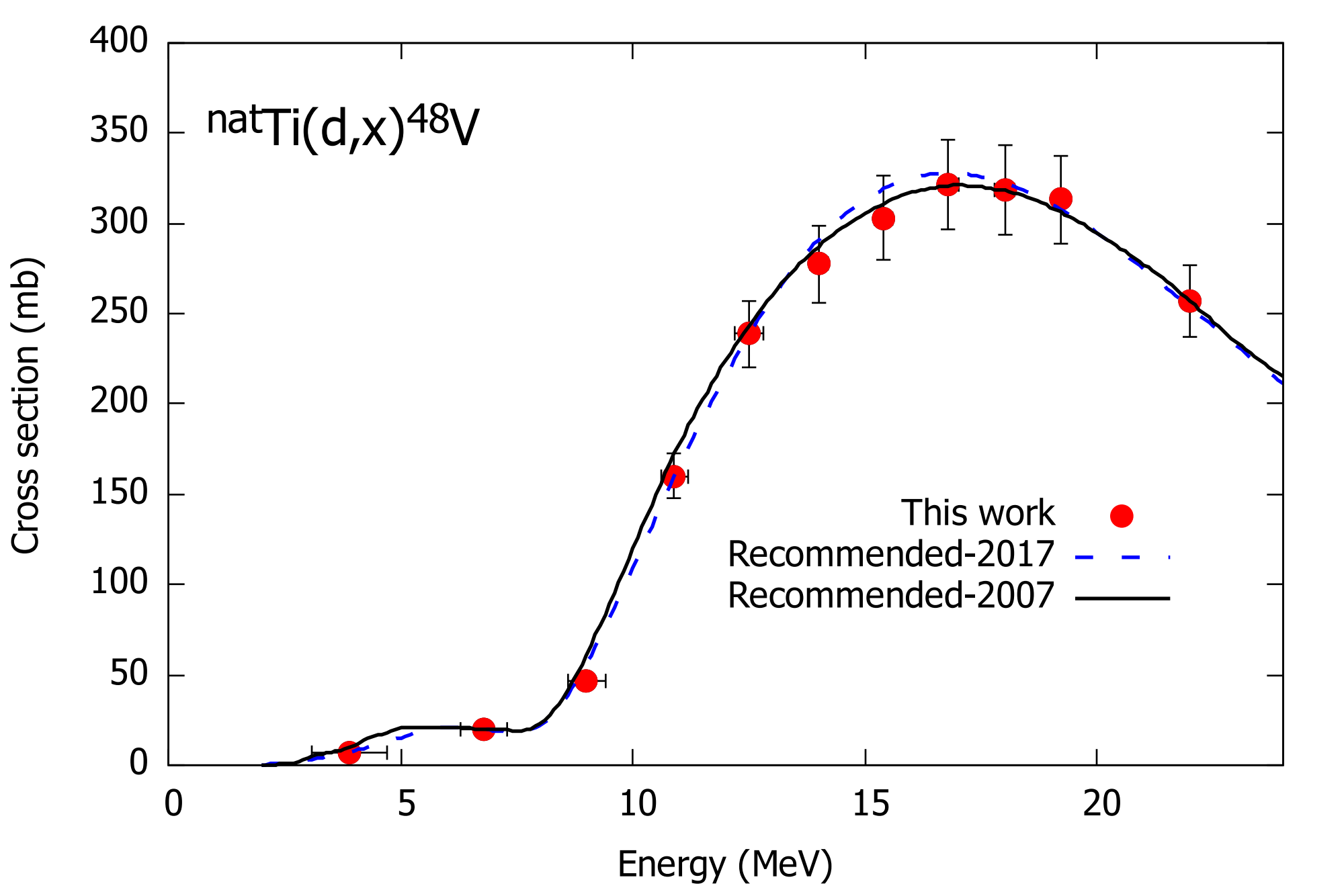
$^{nat}Ti(d,x)^{48}V$
Cross section (mb)
Energy (MeV)
0
50
100
150
200
250
300
350
400
0
5
10
15
20
This work
Recommended-2017
Recommended-2007

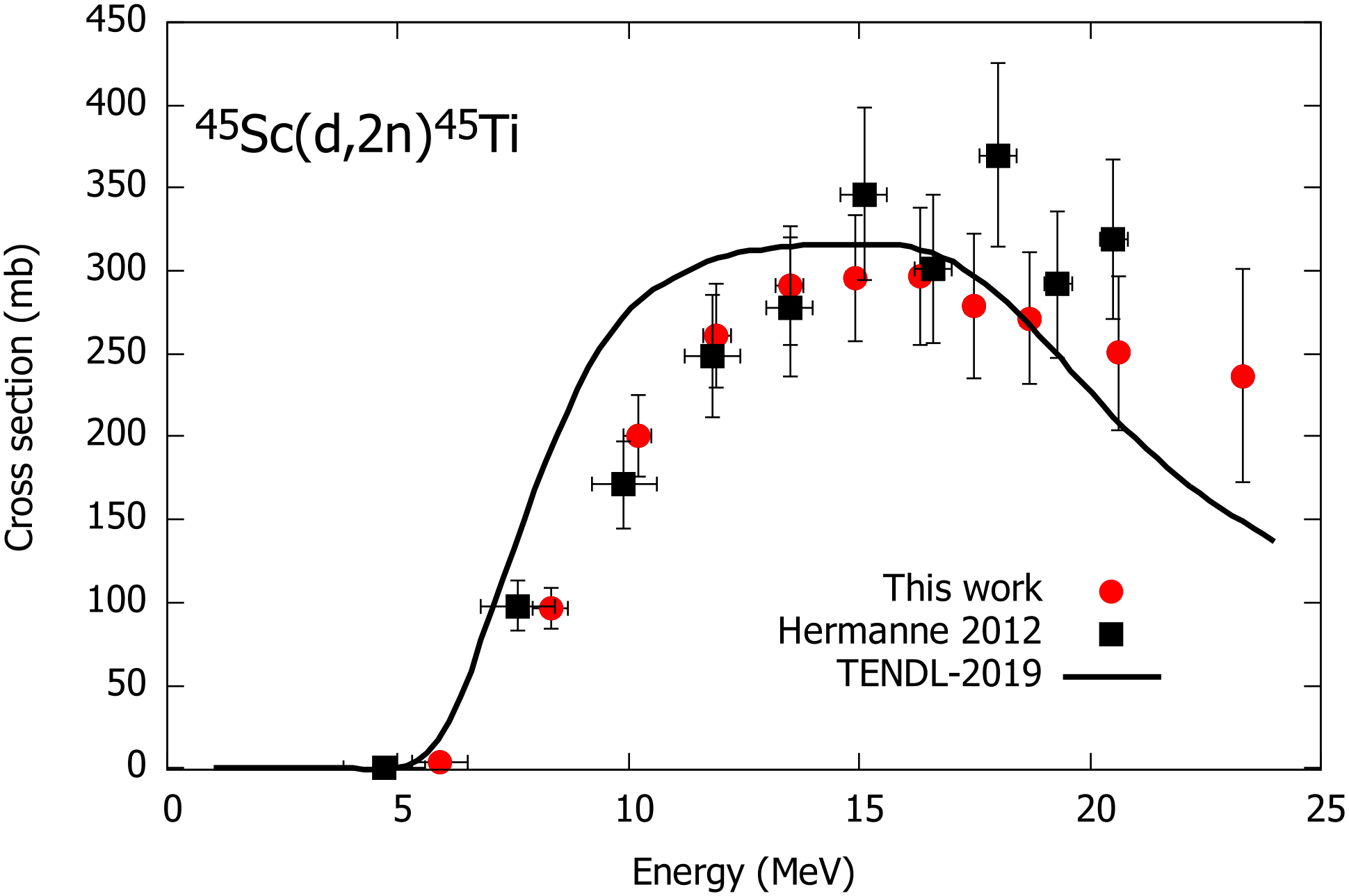
^{45}Sc(d,2n)^{45}Ti
Cross section (mb)
Energy (MeV)
0
50
100
150
200
250
300
350
400
450
0
5
10
15
20
25
This work
Hermanne 2012
TENDL-2019

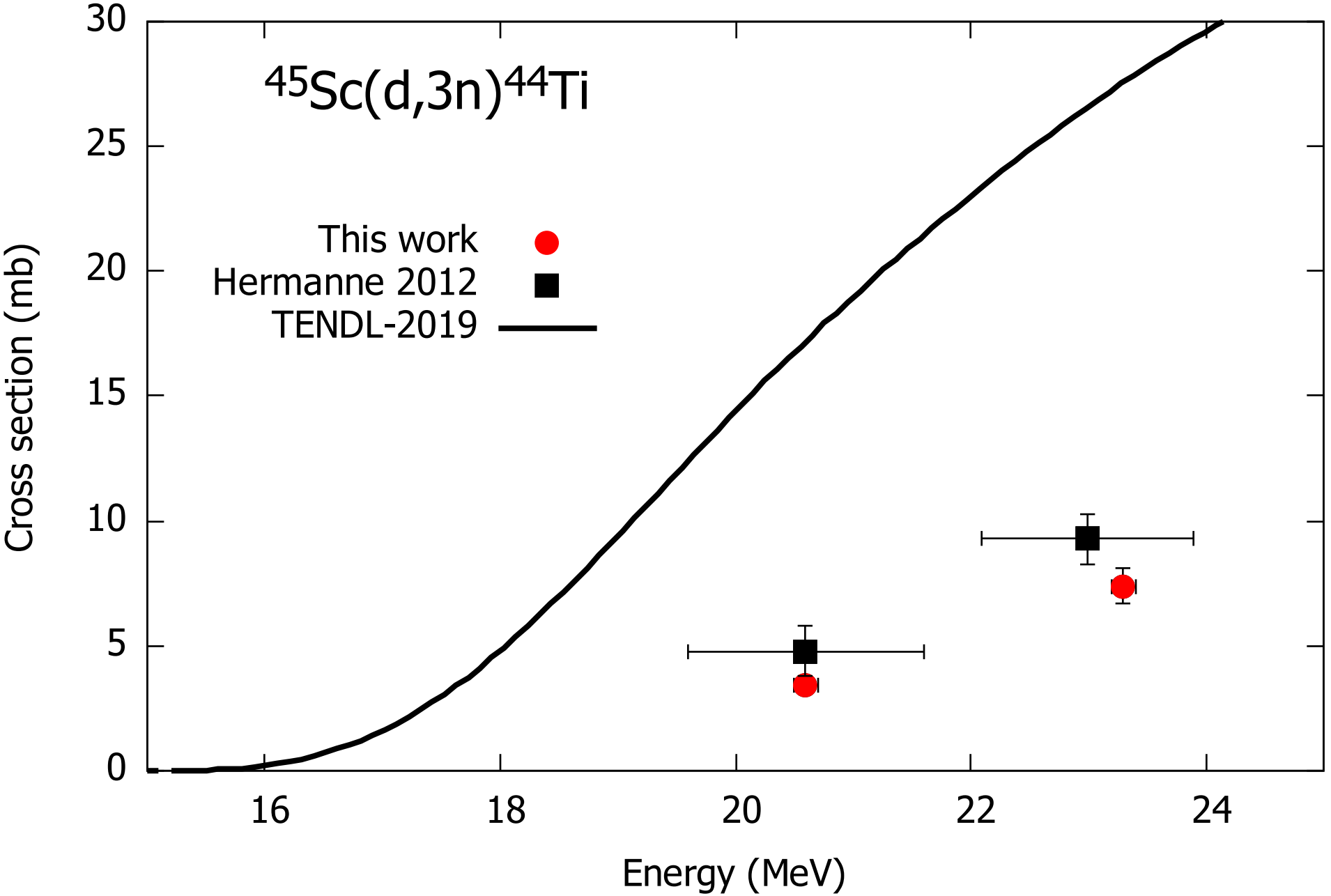
^{45}Sc(d,3n)^{44}Ti
This work
Hermanne 2012
TENDL-2019
Cross section (mb)
Energy (MeV)
0
5
10
15
20
25
30
16
18
20
22
24

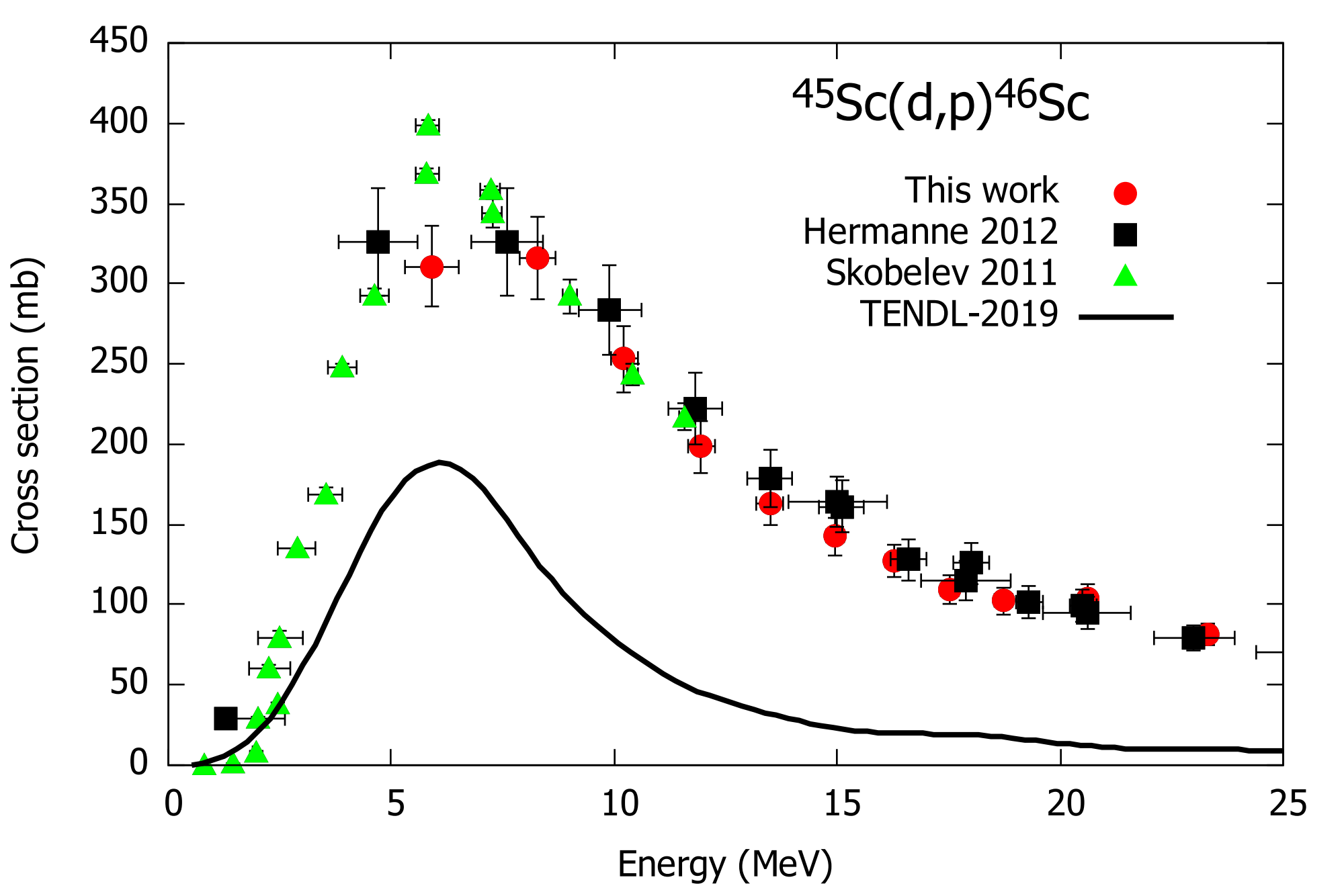
^{45}Sc(d,p)^{46}Sc
This work
Hermanne 2012
Skobelev 2011
TENDL-2019
Cross section (mb)
Energy (MeV)
0
50
100
150
200
250
300
350
400
450
0
5
10
15
20
25

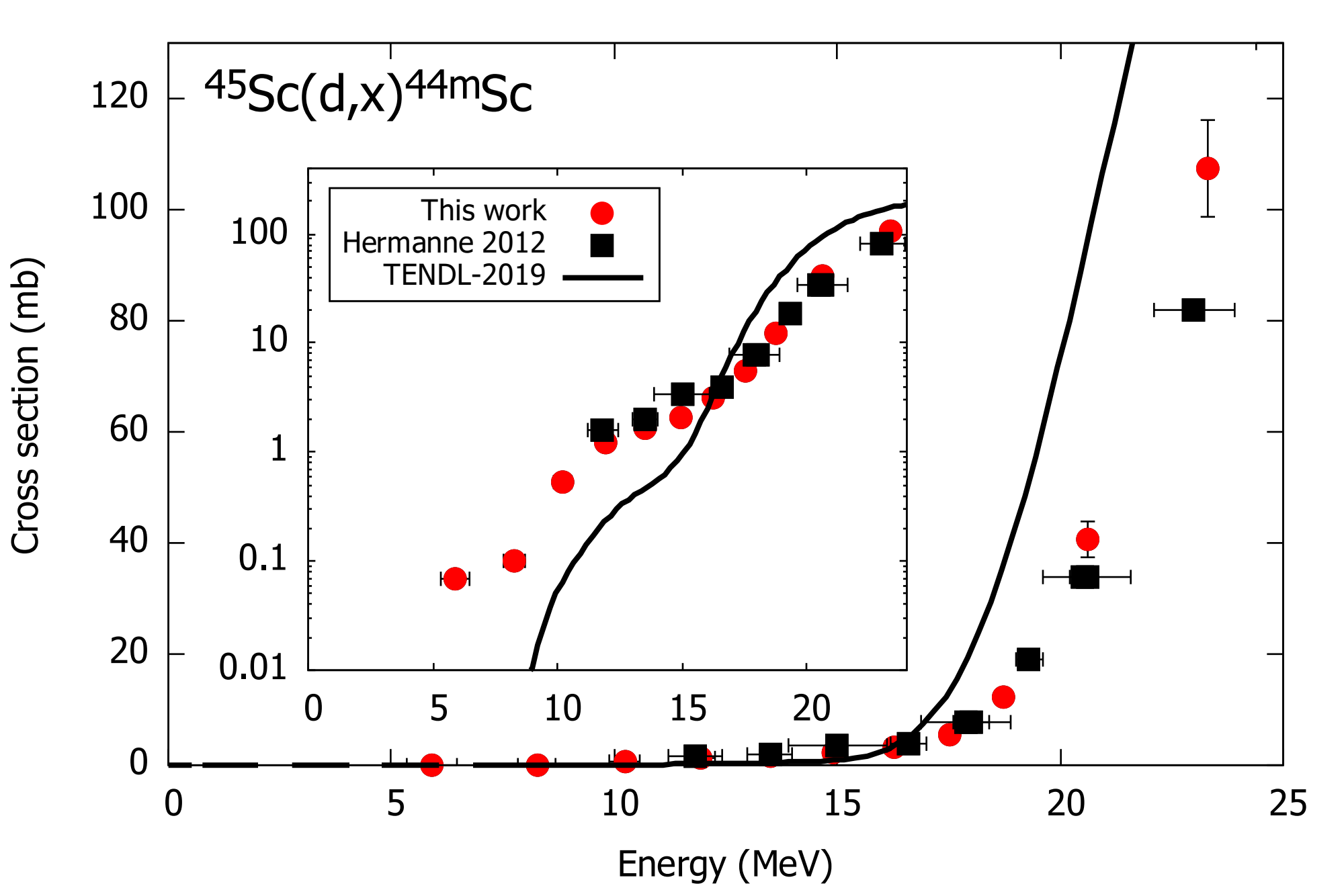
^{45}Sc(d,x)^{44m}Sc
This work
Hermanne 2012
TENDL-2019
Cross section (mb)
Energy (MeV)
0
20
40
60
80
100
120
0
5
10
15
20
25
0.01
0.1
1
10
100

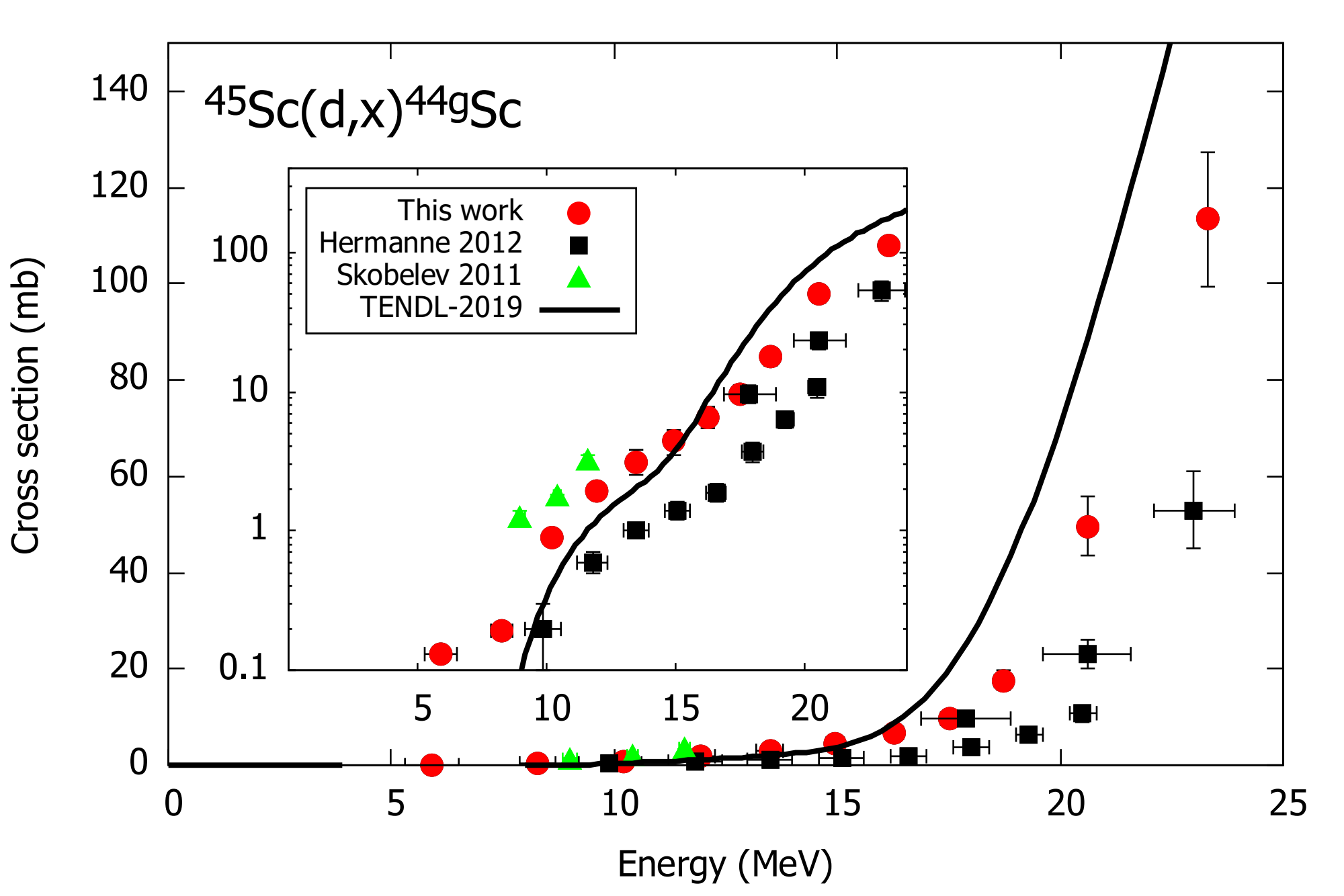
^{45}Sc(d,x)^{44g}Sc
This work
Hermanne 2012
Skobelev 2011
TENDL-2019
Cross section (mb)
Energy (MeV)
0
20
40
60
80
100
120
140
0
5
10
15
20
25
0.1
1
10
100

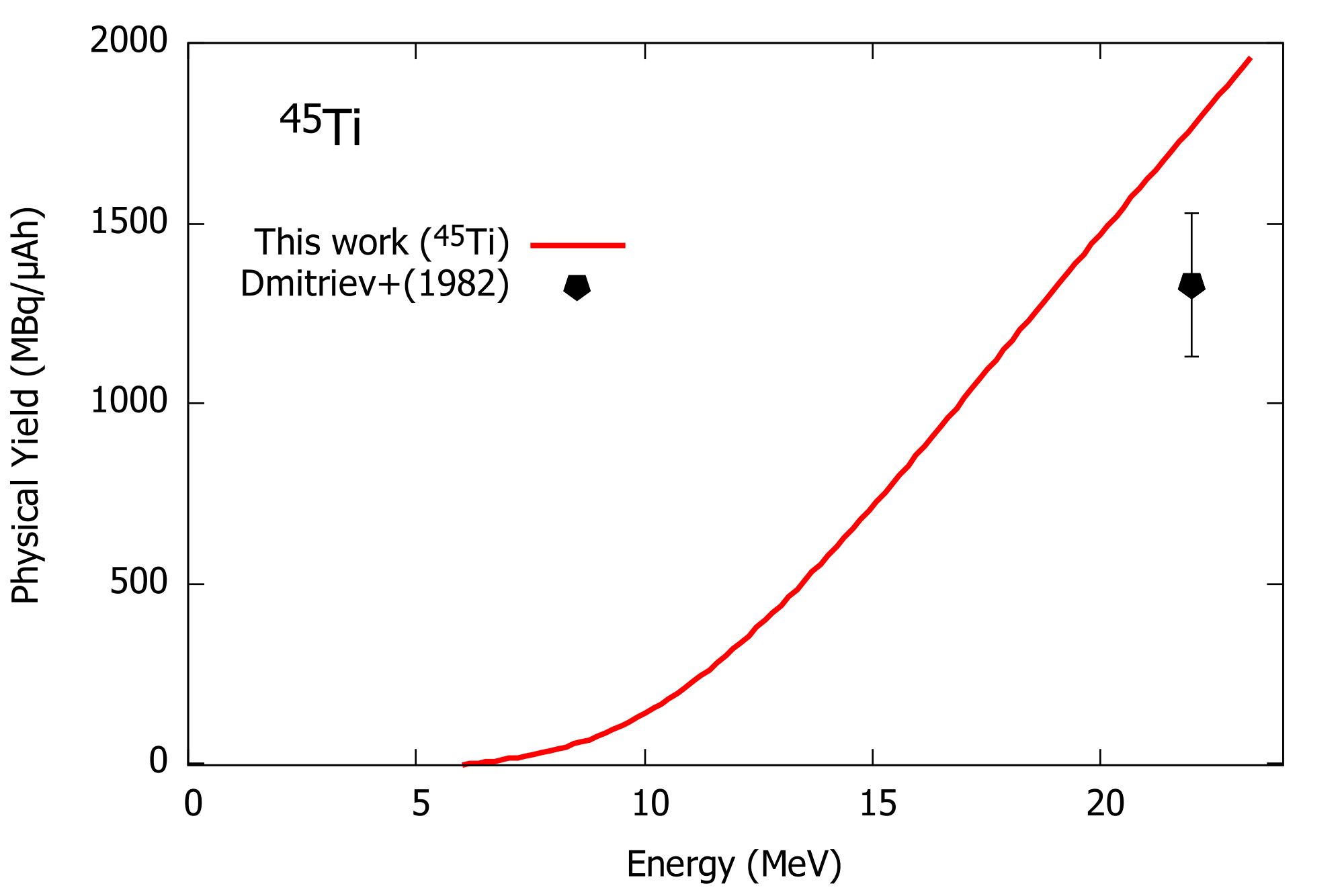
^{45}Ti
This work (^{45}Ti)
Dmitriev+(1982)
Physical Yield (MBq/μAh)
Energy (MeV)
0
500
1000
1500
2000
0
5
10
15
20